

# Reinforcement learning approach to non-equilibrium quantum thermodynamics

Sofia Sgroi,<sup>1,2</sup> G. Massimo Palma,<sup>1,3</sup> and Mauro Paternostro<sup>2</sup>

<sup>1</sup>*Dipartimento di Fisica e Chimica - Emilio Segrè ,  
Università degli Studi di Palermo, via Archirafi 36, I-90123 Palermo, Italy*

<sup>2</sup>*Centre for Theoretical Atomic, Molecular and Optical Physics,  
School of Mathematics and Physics, Queen's University Belfast, Belfast BT7 1NN, United Kingdom*

<sup>3</sup>*NEST, Istituto Nanoscienze-CNR, Piazza S. Silvestro 12, 56127 Pisa, Italy*

(Dated: April 11, 2024)

We use a reinforcement learning approach to reduce entropy production in a closed quantum system brought out of equilibrium. Our strategy makes use of an external control Hamiltonian and a policy gradient technique. Our approach bears no dependence on the quantitative tool chosen to characterize the degree of thermodynamic irreversibility induced by the dynamical process being considered, require little knowledge of the dynamics itself and does not need the tracking of the quantum state of the system during the evolution, thus embodying an experimentally non-demanding approach to the control of non-equilibrium quantum thermodynamics. We successfully apply our methods to the case of single- and two-particle systems subjected to time-dependent driving potentials.

The design, development, and optimization of quantum thermal cycles and engines is one of the most active and attention-catching research strand in the burgeoning field of quantum thermodynamics [1–4]. Besides being one of the most important applications of thermodynamics, thermal engines play also a fundamental role in the development of the theory of classical thermodynamics itself. It is thus not surprising that the community working in the field that explores the interface between thermodynamics and quantum dynamics is very interested in devising techniques for the exploitation of quantum advantages for the sake of realizing quantum cycles and machines [3–5]. The overarching goal is to operate at much smaller scales than classical motors and engines and enhance the performance of such devices so as to reach classically unachievable efficiencies [1, 6–8].

However, the quasi-static approximation that allows us to describe thermodynamic transformations with a relatively simple equilibrium theory does not hold for real thermal engines, which operate in a finite time interval, and thus in explicit non-equilibrium conditions. This is even more the case for sought-after quantum engines: in order to exploit the potential benefits of quantum coherences, such devices should operate within the coherence time of the physical platforms used for their embodiment, which might be very short [5, 9, 10]. Any finite-time process gives rise to a certain degree of thermodynamic irreversibility, as quantified by entropy production, which enters directly into the thermodynamic efficiency of the process, limiting it. Therefore, the effective control of non-equilibrium quantum systems is an important goal to achieve in order to enhance the efficiency of quantum thermal engines [11].

In the case of a closed system, a well-known quantum control approach consists of the use of shortcuts-to-adiabaticity (STA) [12, 13]. While this approach has already been successfully applied to various platforms [14–20], and the possible application of STA to

non-equilibrium thermodynamics has been explored [11, 21–26] it certainly bears considerable disadvantages as it requires extensive knowledge of the system dynamics and, for this reason, it is difficult to use it as an on-the-run experimental procedure. Moreover, STA techniques do not allow for the choice of the function that characterizes the dissipative processes for the system and it is currently very difficult to incorporate in a working STA protocol any constraint on the energetic cost of its implementation [27, 28]. This is why alternative approaches are necessary to improve our understanding and control power over quantum systems that are subjected to a non-equilibrium processes.

A possible approach to address this problem is to make use of machine learning techniques that are currently being employed in growing number of problems. In particular, quantum physics is benefiting from machine learning techniques in many ways in light of their capability to approximate high dimensional functions that would be difficult to infer otherwise. Numerous applications have been developed, ranging from phase detection [29, 30] to the simulation of stationary states of open quantum many body systems [31], from the research of novel quantum experiments [32] to quantum protocols design [33, 34], from the learning of states and operations [35, 36] to the modelling and reconstruction of non-Markovian quantum processes [32, 37] and the engineering of non-classical states useful for quantum computing [38, 39]. In general, classification or regression problems are best tackled via supervised-learning approaches, while unsupervised-learning techniques are beneficial for the inference of patterns from data [40]. Finally, problems linked to planning or control can be successfully addressed through reinforcement learning (RL) methods [41].

In this paper, we extend the range of quantum problems that can be successfully tackled with machine learning approaches by demonstrating its successful deploy-

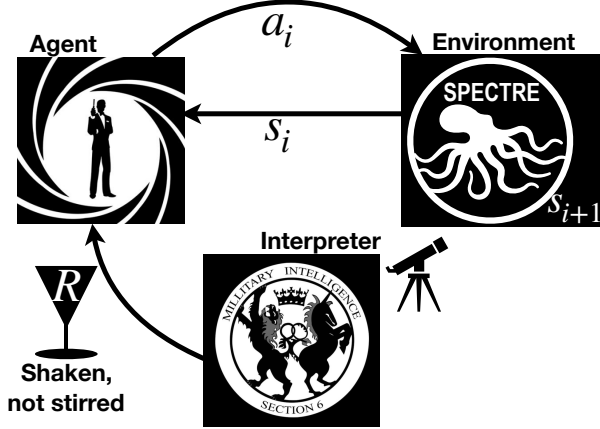


FIG. 1. Scheme of principle of RL: at the  $i^{\text{th}}$  step of the protocol, an agent performs observations on an environment, acquiring its state  $s_i$ , upon which he decides to implement action  $a_i$ . As a result, the state of the environment is updated to  $s_{i+1}$ . Based on the actions of the agent and the states of the environment, an interpreter decides to grant the agent a reward  $R$ , which the latter aims to maximize.

ment to the assessment of non-equilibrium thermodynamics of quantum processes. In particular, we propose an approach to reduce energy dissipation and thermodynamic irreversibility arising from a unitary work protocol using an approach based on RL. Specifically, we make use of as policy gradient technique to tackle out-of-equilibrium work-extraction protocols whose thermodynamic irreversibility we aim at controlling and reducing. Our RL methodology allows us to address this problem with only little knowledge of the system dynamics and to choose how to quantify dissipations. Our study provides a significant contribution to the development of successful control strategies tailored for physically relevant non-equilibrium quantum processes, thus complementing the scenario drawn so far and based on optimal control and STA methods.

The remainder of this manuscript is organized as follows. In Sec. I we introduce the RL setting upon which our approach is based. In Sec. II we present our approach to the control and optimization of non-equilibrium work extraction protocols, while Secs. III and III B are dedicated to the illustration of such methodology through simple yet physically significant examples. Finally, in Sec. IV we draw our conclusions and briefly discuss potential avenues of expansion of our research lines.

## I. BACKGROUND ON REINFORCEMENT LEARNING

Here we provide a short account of the RL framework that will be exploited to tackle non-equilibrium thermodynamics illustrated in Sec. II.

In the RL setting, an agent dynamically interacts with an environment and learns from such interaction how to behave in order to maximize a given reward functional [41, 42]. The process is typically divided in discrete interaction steps: at each step  $i$ , the agent makes an observation of the environment state  $s_i$  and – based on the outcomes of their observations – takes an action  $a_i$ . Based on this action, the environment state is updated to  $s_{i+1}$  and we repeat the procedure for the new step  $i + 1$ . This is iterated for a given number of steps or until we reach a certain state, when a third party (an interpreter) provides the agent with a reward  $R(s_0, a_0, s_1, a_1, \dots)$ . Based on their past behaviour and the states of the environment, the agent change the way further actions are chosen so as to maximize the future values of the reward (cf. Fig. 1). This procedure is repeated for a certain number of epochs until, if possible, the agent learn how to reach the maximum reward.

If the environment is completely observable, at each step the agent action and the reward depend only on the observation at the current step and the process is said to be a Markov decision process (MDP). In this case, we can describe the behaviour of the agent using a policy function  $\pi(a_i|s_i)$ . This represents the probability for the agent to choose the action  $a_i$ , given the state  $s_i$  of the environment. In a policy gradient approach, we parametrize the policy function  $\pi_{\theta}(a_i|s_i)$  with a set of parameters  $\theta$ , and change them accordingly to the reward. This can be done using a gradient ascent algorithm. If the reward is given to the agent at the end of each epoch, as in our case, the gradient ascent reads [43]

$$\Delta\theta = \eta R \sum_{a_i} \nabla_{\theta} \log \pi_{\theta}(a_i, s_i), \quad (1)$$

where  $\eta$  is a parameter known as “learning rate” and the sum is calculated over the actions taken in any given *trajectory*  $\{a_i\}_i$ .

For a continuous action space, we assume a certain shape for the policy function and we use a function approximator for one or more parameters of the probability distribution [41]. Here we assume the policy function to be a Gaussian and take

$$\pi_{\theta}(a_i|s_i) = \frac{1}{\sigma \sqrt{2\pi}} e^{-\frac{(a_i - \mu_{\theta}(s_i))^2}{2\sigma^2}}, \quad (2)$$

where we treat  $\sigma$  as an external parameter and we use a neural network for the parametrization of  $\mu$ . We further introduce a parameter  $\epsilon$  such that, at each step, with a probability  $\epsilon$ , the agent takes a completely random action from a uniform distribution, ignoring the policy in Eq. (2). This reduces the possibility for the agent to get stuck in a local maximum and leads to a better exploration of the space of possible actions.

Based on our choice for  $\pi_{\theta}(a_i|s_i)$  made in Eq. (2), the condition in Eq. (1) is satisfied if the neural network is

trained with a stochastic gradient descent method over the batch using the cost function

$$C = \frac{1}{2\sigma^2} \sum_{a_i} R |a_i - \mu_{\theta}(s_i)|^2. \quad (3)$$

## II. PHYSICAL SYSTEM AND METHODOLOGY

Let us consider a closed quantum system evolving under a time dependent Hamiltonian  $H_S(t)$  within the time interval  $[0, \tau]$ . We want to control the system evolution using an additional Hamiltonian  $H_{\text{opt}}(t)$  such that  $H_{\text{opt}}(0) = H_{\text{opt}}(\tau) = 0$ .

For simplicity, we consider  $H_{\text{opt}}(t) = f_{\text{opt}}(t)M_{\text{opt}}$  where the operator  $M_{\text{opt}}$  is kept fixed and we control the function  $f_{\text{opt}}(t)$  (enforcing the boundary conditions  $f_{\text{opt}}(0) = f_{\text{opt}}(\tau) = 0$  so as to fulfil the requests made on the Hamiltonian) to optimize the process. The total Hamiltonian of the system during its evolution is thus

$$H(t) = H_S(t) + f_{\text{opt}}(t)M_{\text{opt}}. \quad (4)$$

We divide the system evolution in a certain number of discrete time steps. At each step  $t_i$ , the agent makes an observation  $s_i$  and chooses an action  $a_i$ . This is done by extracting a random number according to Eq. (2), based on the prediction of the neural network for  $\mu_{\theta}(s_i)$ . We then take the function  $f_{\text{opt}}(t) = a_i$  in the interval  $[t_i, t_{i+1}]$ . We limit the maximum and the minimum output of the network  $|\mu_{\theta}(s_i)| < \mu^*$  so that we can control the maximum amount of energy spent for the optimization. This is important when we deal with thermal engines, as we do not want to spend more energy for the control than the amount that we extract from the process. This process is done in parallel for a batch of systems and, at the end of the evolution, the neural network is trained on this batch and the corresponding rewards. The procedure is repeated for a certain number of epochs, each time resetting the system and the Hamiltonian to the original state and value. The process is then run again and the best  $f_{\text{opt}}(t)$  is chosen as the one that maximize the reward over the batch.

We now comment on the quantifier of irreversibility addressed in our study and the different approaches that we will consider to reduce the system dissipations. The first approach aims to reduce the mean entropy production of the system [1, 44–48], calculated as the relative entropy between the final state of the system  $\rho(\tau)$  and the corresponding instantaneous thermal equilibrium state  $\rho^{eq}(t) = e^{-\beta H_S(t)}/Z_S(t)$  with  $Z_S(t) = \text{tr}[e^{-\beta H_S(t)}]$  being the partition function of the system. We thus consider the quantity

$$\Sigma = S(\rho(\tau) \parallel \rho^{eq}(\tau)) \quad (5)$$

where  $S(\sigma \parallel \chi) = \text{tr}[\sigma(\log \sigma - \log \chi)]$  is the quantum relative entropy [49]. For this purpose, we use a Dense-layers Neural Network [50] that takes as inputs the time

step and the density matrix of the system. In this case, the agent reward is

$$R = -\Sigma, \quad (6)$$

which is perfectly suited to our goal: the agent gets rewarded by reducing the degree of irreversibility of the process.

In the second approach, we assume to take a measurement of the energy of the system before the evolution [51, 52]. We consider the simple case in which the energy levels are not degenerate and we use as reward the squared root of the fidelity between the final state of the system and the corresponding adiabatic final state. Then we have

$$R = |\langle \phi(t) | \phi_{ad}(t) \rangle|. \quad (7)$$

This approach too benefits of the use of a Dense-layers Neural Network with inputs embodied by the time step and the (pure) quantum state of the system.

The third approach makes use of the same ideas laid out above. However, this time we want the model to be useful as a control technique even when we are not able to simulate or track the dynamics of the system. We thus use a different input, while still considering a MDP. We use a Long-Short-Term-Memory (LSTM) Neural Network [43] that takes as inputs the energy measured at the beginning of the evolution, and the time steps.

If the observation of our agent at a given time step contains all the informations about the initial state of the system and the control term of the Hamiltonian at any previous time, the knowledge of the current quantum state is no longer required in order to have a MDP. However, we can avoid to use such a large input at each step if we use a LSTM network instead. The output of a LSTM network does not only depend on the input at a given time step, but also on all the previous inputs and outputs. These kind of neural networks are indeed capable of memorizing long term dependencies and are widely used today for those tasks that involve sequential data, such as speech recognition.

For these reasons, we just need to take measurements at the beginning and at the end of the evolution. Needless to say, this embodies a significant reduction on the practical complexity of the control protocol, as the scheme only requires two measurements, and thus leaves room for a non-demanding experimental implementations that does not need to track the evolution of the system.

Should the initial state of the system be inaccessible, or should we want to avoid performing a measurement at the start of the dynamics, if we assume the initial density matrix of the system to be always the same, we can still use a LSTM network in a way similar to the first approach, with just the time steps as inputs and a reward given by Eq. (6).

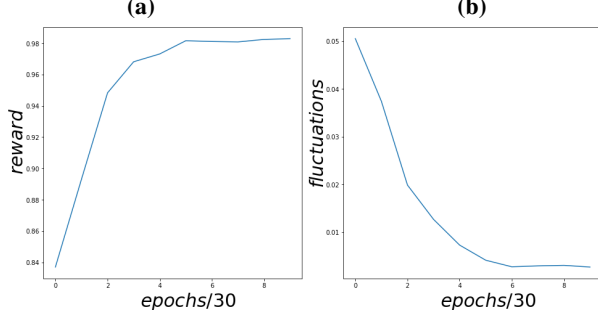


FIG. 2. In panel (a) we show the average reward over the batch and 30 epochs as a function of the number of epochs of training. Panel (b) shows the associate fluctuations. From the asymptotic behavior of both curves we see that the training is successfully achieved.

### III. CASE STUDIES

We now apply the methods highlighted in Secs. I and II using simple yet physically relevant physical models. Specifically, we will address the cases of a single spin-like system exposed to a time-dependent field and a model of two spins coupled with a time-dependent Hamiltonian.

#### A. Single spin-1/2 particle in a time-dependent field

Let us consider the simple model of a qubit evolving in the interval  $t \in [0, \tau]$  under an Hamiltonian (we consider units such that  $\hbar = 1$  throughout this paper)

$$H_S(t) = [\sigma_x B_x(t) + \sigma_z B_z(t)] / 2 \quad (8)$$

with  $B_x^2(t) + B_z^2(t) = B_0^2 \forall t \in [0, \tau]$ , thus modelling a spin subjected to a rotating magnetic field. We assume that the system is initialized in a thermal state at inverse temperature  $\beta$ . This is relevant only when we do not take an energy measurement at the beginning of the evolution.

Our optimization Hamiltonian is  $H_{opt}(t) = -f_{opt}(t)\sigma_y$  so that  $H(t) = H_S(t) - f_{opt}(t)\sigma_y$ .

We start with the first approach, introduced in the previous section, that aims to reduce the relative entropy (Eq. 5). We introduce the entropy production reduction

$$\Delta\Sigma = 1 - \frac{\Sigma_{opt}}{\Sigma_{free}}, \quad (9)$$

where  $\Sigma_{opt}$  is the entropy production [cf. Eq. (5)] and  $\Sigma_{free}$  is the entropy production of the same systems without the optimization term in the Hamiltonian.

Likewise, the reduction of the work done on the systems will be defined as

$$\Delta W = 1 - \frac{\Delta U_{opt} + E_{in}}{\Delta U_{free}}, \quad (10)$$

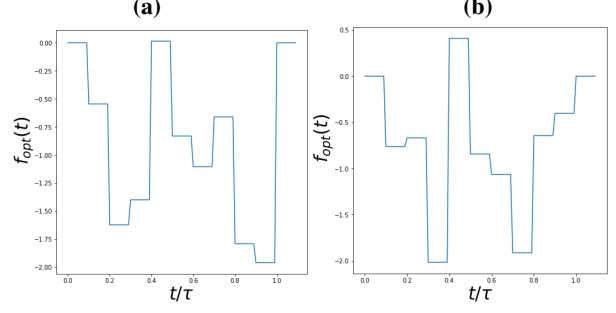


FIG. 3. We show the form taken by  $f_{opt}(t)$  for two different runs of the optimization process. Although they both reduce the entropy production of approximately the same amount (99.86% in panel (a) and 99.80% in panel (b) respectively), the trends followed by the control function are visibly different.

where  $E_{in}$  is an estimation of the energy spent for the optimization, defined as [21]

$$E_{in} = \left| \int_0^1 \text{tr}(\rho(t)f_{opt}(t)\sigma_y) dt \right|. \quad (11)$$

and  $\Delta U$  is the variation on the internal energy  $U(t) = \text{tr}(\rho(t)H(t))$  of the system between the initial and the final state.

When using the second approach to the quantification of irreversibility, we gain additional information about the system in light of the fact that our control process starts only after a measurement. Our  $f_{opt}(t)$  is then dependent on the initial state. Based on our knowledge of the initial pure state of the system, we want to make the final state as close as possible to the adiabatic one (that is, the corresponding eigenvector of  $H_S(\tau)$ ). Therefore our measure for the performance of this approach will be the fidelity of the final state with the adiabatic target  $|\langle \phi(\tau) | \phi_{ad}(\tau) \rangle|^2$ .

For the third approach, we again solve the previous problem but this time with a LSTM Neural Network, as discussed in Sec. II.

#### 1. Hyperparameters and numerical results

We divided the dynamics of our system in 10 steps and set  $\mu^* = 3$ ,  $\sigma = 1$ . We also fixed  $\epsilon = 0.1$  up to the last set

	$J(t)$	$\Sigma_{lib}/\beta$	$\Sigma_{opt}/\beta$	$\Delta U_{lib}$	$\Delta U_{opt}$	$E_{in}$
Eq. (15)	0.600644	0.370925	0	-0.229719	0.001515	
Eq. (16)	0.575289	0.370684	-0.025354	-0.229959	0.000954	

TABLE I. Numerical results for a simulation of the free and of the optimized evolution for the different choices of  $J(t)$  made in the text. We notice that the optimized quantities are very close for both the different interaction term functions. In both cases, we achieved an error of  $10^{-6}$ .

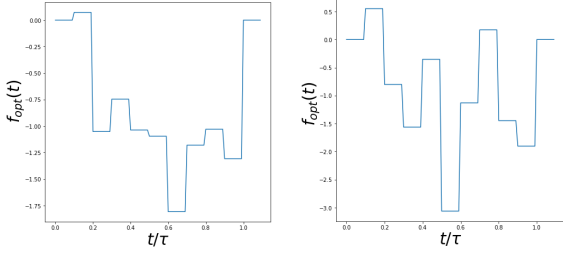


FIG. 4. From the left, example of  $f_{opt}(t)$  for an initial up and down state of  $H_S(0)$ , respectively. The corresponding fidelity with the targets is 0.997.

of 100 epochs, and then set it to zero. Our Dense-layers Neural Network had 3 hidden layers of 100 neurons and used a Rectified Linear Unit activation function, while our LSTM Neural Network consisted in 50 LSTM units followed by a 30 neurons dense layer with a Hyperbolic Tangent activation function. For both networks we set the activation function of the final layer to be a Hyperbolic Tangent, so that we could fix the maximum output value.

We started taking  $B_x(t) = B_0 \sin(\frac{\pi t}{2\tau})$  in [cf. Eq. (8)].

For each of the methods described in Sec. II, we ran 20 simulations of a training consisting in 300 epochs with a batch of 30 systems. In Fig. 2 we show a typical example of a learning curve, indicating that the training was successfully achieved.

Using the first approach with an initial thermal state with  $\beta = 1$ , we successfully reduced both the relative entropy  $\Delta\Sigma = (99 \pm 1)\%$  and the work done on the system  $\Delta W = (91 \pm 9)\%$ . Examples of  $f_{opt}(t)$  are given in Fig. 3.

When the second approach to irreversibility was used, we obtained a fidelity with the adiabatic target  $F_{ad}(\tau) = |\langle \phi(\tau) | \phi_{ad}(\tau) \rangle|^2$  as large as  $F_{ad}(\tau) = 0.997 \pm 0.002$ . In Fig. 4 we show an example of  $f_{opt}(t)$  for this case. Finally, for the third approach we successfully obtained  $F_{ad}(\tau) = 0.998 \pm 0.001$  as fidelity with the adiabatic target state.

We have rounded our analysis by running a single simulation for a different choice of time-dependent field. We thus set  $B_x(t) = B_0 \sin[\frac{\pi}{2} \sin^2(\frac{\pi t}{2\tau})]$ , obtaining a value of the adiabatic fidelity as large as  $F_{ad}(\tau) \approx 0.998$ . The corresponding functions  $f_{opt}(t)$  are shown in Fig. 5.

## B. Time-dependent coupling of spin-1/2 particles

Let us now consider a slightly more complicated system composed of two two-level systems interacting according to the Hamiltonian

$$H_S(t) = \sigma_z^1 \otimes I^2 + \frac{1}{2} I^1 \otimes \sigma_z^2 + J(t)(\sigma_+^1 \otimes \sigma_-^2 + \sigma_+^2 \otimes \sigma_-^1), \quad (12)$$

where the coupling strength  $J(t)$  evolves in the time interval  $t \in [0, \tau]$ .

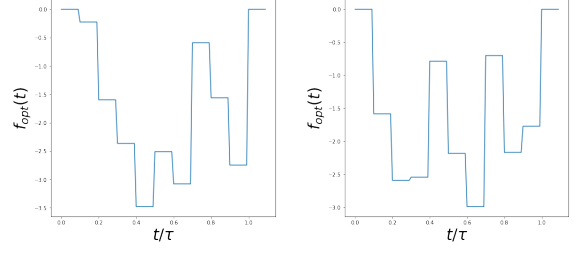


FIG. 5. From the left, example of  $f_{opt}(t)$  for an initial up and down state of  $H_S(0)$ , respectively. Here  $B_x(t) = B_0 \sin(\frac{\pi}{2} \sin^2(\frac{\pi t}{2\tau}))$ .

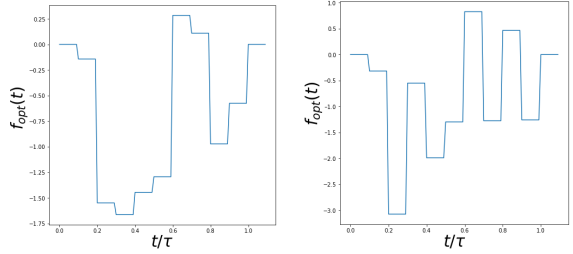


FIG. 6.  $f_{opt}(t)$  for  $J(t) = \chi(t/\tau - 0.5)$  (left) and  $J(t) = \sin(\frac{\pi}{2}(1 - \cos(\pi t/2\tau)))$  (right).

We start with both spins in a thermal state with an inverse temperature  $\beta$ . Our control term is

$$H_{opt}(t) = (\sigma_x^1 \otimes \sigma_y^2 + \sigma_y^2 \otimes \sigma_x^1) f_{opt}(t). \quad (13)$$

We aim at reducing the relative entropy [cf. Eq. (5)], this time using a LSTM Neural Network, as described at the end of Sec. II.

As we must have the same variation in the Helmholtz free energy between the initial and final state [44, 46, 47]

$$\Delta F = \Delta U - \frac{\Sigma}{\beta}, \quad (14)$$

for both the free and the optimized process, we set the error in our energy measurements to be the difference in this quantity for the two processes.

### 1. Hyperparameters and numerical results

We divided the dynamics of our system in 10 steps and fixed  $\mu^* = 5$ ,  $\sigma = 1$  and  $\epsilon = 0.1$  until the last 100 epochs, then we set  $\epsilon = 0$ . We used a batch of 30 systems and considered 300 epochs.

Again, our LSTM Neural Network consisted of a LSTM layer with 50 units, followed by a 30 neurons dense layer and a single output neuron with a Hyperbolic Tangent activation function.

We ran a simulation with a choice of time-dependent coupling rate as

$$J(t) = \chi\left(\frac{t}{\tau} - 0.5\right) \quad (15)$$

with  $\chi(t - t_0)$  the step function taking unit value at  $t = t_0$  and being null otherwise. We have also considered the case of

$$J(t) = \sin\left[\frac{\pi}{2} - \frac{\pi}{2} \cos\left(\frac{\pi t}{2\tau}\right)\right], \quad (16)$$

both for an initial thermal state with  $\beta = 1$ .

Our results are shown in Fig. 6 and Table I. A successful reduction of entropy production is achieved in both cases. Moreover we see that the entropy production  $\Sigma_{opt}$  for both the optimized processes takes very similar values. Similar considerations hold for  $\Delta U_{opt}$ . This is encouraging, although not surprising as for both processes we have  $J(0) = 0$  and  $J(\tau) = 1$  so that the corresponding adiabatic process is the same, and we have, in fact, the same  $\Delta F$ .

Next, using Eq. (15), we changed the temperature of the initial state of the system in the range  $\beta \in [0.1, 2.1]$ , dividing this interval in 20 steps. Running a single simulation for each of these values of  $\beta$ , we obtained a mean entropy production reduction  $\Delta\Sigma \approx 28\%$  in this interval.

#### IV. CONCLUSIONS

We have proposed and benchmarked a technique based on a deep RL approach to reduce the degree of irreversibility resulting from a non-equilibrium thermodynamic transformation of a closed quantum system. Our method can be used with an arbitrary choice of the function that characterizes the dissipative process undergone by the system and requires very scanty knowledge of the

system dynamics. Moreover, it can be applied even without tracking the state of the system during the evolution, thus opening the doors for non-demanding experimental implementations.

We applied our technique to two simple yet relevant physical models. Namely we successfully reduced the entropy production and the distance of the final state from the adiabatic target for a spin-1/2 particle subjected to a time-dependent magnetic field and the entropy production resulting from the time-dependent coupling between two spin-1/2 particles. While we focused on simple models for the development of the technique, and as our approach should not be affected by the system dimension and complexity, it would be interesting to apply it to a many-body quantum system. Needless to say, both the hyperparameters and the number of epochs needed for the training would have to be suitably tailored. This could help significantly in the development of an efficient mesoscopic thermal engine operating under realistic conditions. A natural further development of our work would be the extension to open quantum systems dynamics.

#### ACKNOWLEDGMENTS

SS thanks the Centre for Theoretical Atomic, Molecular, and Optical Physics, School of Mathematics and Physics, Queen's University Belfast for hospitality during the initial phases of this work. We acknowledge support from the H2020-FETOPEN-2018-2020 TEQ (grant nr. 766900), the DfE-SFI Investigator Programme (grant 15/IA/2864), COST Action CA15220, the Royal Society Wolfson Research Fellowship (RSWF\R3\183013), the Leverhulme Trust Research Project Grant (grant nr. RGP-2018-266), the PRIN project 2017SRN-BRK QUSHIP funded by MIUR.

- 
- [1] S. Vinjanampathy and J. Anders, *Contemp. Phys.* **57**, 545 (2016).
  - [2] S. Deffner and S. Campbell, *Quantum Thermodynamics* (Morgan and Claypool Publishers, 2019).
  - [3] M. T. Mitchison, *Contemp. Phys.* **60**, 164 (2019).
  - [4] R. Kosloff and A. Levy, *Annual Review of Physical Chemistry* **65**, 365 (2014).
  - [5] G. Barontini and M. Paternostro, *New Journal of Physics* **21**, 063019 (2019).
  - [6] W. Niedenzu, V. Mukherjee, A. Ghosh, A. G. Kofman, and G. Kurizki, *Nat. Comm.* **9** (2018).
  - [7] B. K. Agarwalla, J.-H. Jiang, and D. Segal, *Phys. Rev. B* **96**, 104304 (2017).
  - [8] J. Klaers, S. Faelt, A. Imamoglu, and E. Togan, *Phys. Rev. X* **7**, 031044 (2017).
  - [9] D. von Lindenfels, O. Gräß, C. T. Schmiegelow, V. Kaushal, J. Schulz, M. T. Mitchison, J. Goold, F. Schmidt-Kaler, and U. G. Poschinger, *Phys. Rev. Lett.* **123**, 080602 (2019).
  - [10] J. P. S. Peterson, T. B. Batalhão, M. Herrera, A. M. Souza, R. S. Sarthour, I. S. Oliveira, and R. M. Serra, *Phys. Rev. Lett.* **123**, 240601 (2019).
  - [11] A. del Campo, J. Goold, and M. Paternostro, *Sci. Rep.* **4**, 6208 (2014).
  - [12] E. Torrontegui, S. Ibáñez, S. Martínez-Garaot, M. Modugno, A. del Campo, D. Guéry-Odelin, A. Ruschhaupt, X. Chen, and J. G. Muga, *Adv. At. Mol. Opt. Phys.*, edited by E. Arimondo, P. R. Berman, and C. C. Lin, Vol. 62 (Academic Press, 2013) p. 117.
  - [13] M. V. Berry, *J. Phys. A: Math. Theor.* **42**, 365303 (2009).

- [14] D. Guéry-Odelin, A. Ruschhaupt, A. Kiely, E. Torrontegui, S. Martínez-Garaot, and J. G. Muga, *Rev. Mod. Phys.* **91**, 045001 (2019).
- [15] M. Palmero, S. Wang, D. Guéry-Odelin, J.-S. Li, and J. G. Muga, *New Journal of Physics* **18**, 043014 (2016).
- [16] H. L. Mortensen, J. J. W. H. Sørensen, K. Mølmer, and J. F. Sherson, *New J. Phys.* **20**, 025009 (2018).
- [17] S. Deng, P. Diao, Q. Yu, A. del Campo, and H. Wu, *Phys. Rev. A* **97**, 013628 (2018).
- [18] F.-H. Ren, Z.-M. Wang, and Y.-J. Gu, *Physics Letters A* **381**, 70 (2017).
- [19] H. Saberi, T. Opatrny, K. Mølmer, and A. del Campo, *Physical Review A* **90** (2014).
- [20] S. Campbell, G. De Chiara, M. Paternostro, G. M. Palma, and R. Fazio, *Phys. Rev. Lett.* **114**, 177206 (2015).
- [21] O. Abah and E. Lutz, *EPL (Europhysics Letters)* **118**, 40005 (2017).
- [22] S. Deng, A. Chenu, P. Diao, F. Li, S. Yu, I. Coulamy, A. del Campo, and H. Wu, *Sci. Adv.* **4** (2018).
- [23] O. Abah and M. Paternostro, *Phys. Rev. E* **99**, 022110 (2019).
- [24] B. Çakmak and Ö. E. Müstecaplıoğlu, *Phys. Rev. E* **99**, 032108 (2019).
- [25] O. Abah and E. Lutz, *Phys. Rev. E* **98**, 032121 (2018).
- [26] O. Abah, M. Paternostro, and E. Lutz, *arXiv:1911.00373* (2019).
- [27] Y. Zheng, S. Campbell, G. De Chiara, and D. Poletti, *Phys. Rev. A* **94**, 042132 (2016).
- [28] A. C. Santos and M. S. Sarandy, *Sci. Rep.* **5**, 15775 (2015).
- [29] P. Broecker, F. Assaad, and S. Trebst, *arXiv:1707.00663* (2017).
- [30] J. Carrasquilla and R. G. Melko, *Nat. Phys.* **13**, 1745 (2017).
- [31] N. Yoshioka and R. Hamazaki, *Phys. Rev. B* **99**, 214306 (2019).
- [32] A. A. Melnikov, H. Poulsen Nautrup, M. Krenn, V. Dunjko, M. Tiersch, A. Zeilinger, and H. J. Briegel, *Proc. Natl. Acad. Sci.* **115**, 1221 (2018).
- [33] R. Porotti, D. Tamascelli, M. Restelli, and E. Prati, *Commun. Phys.* **2**, 2399 (2019).
- [34] I. Paparella, L. Moro, and E. Prati, *Phys. Lett. A* **384**, 126266 (2020).
- [35] L. Innocenti, L. Banchi, A. Ferraro, S. Bose, and M. Paternostro, *arXiv:1903.07119* (2018).
- [36] C. Harney, S. Pirandola, A. Ferraro, and M. Paternostro, *New J. Phys.* **22**, 045001 (2018).
- [37] L. Banchi, E. Grant, A. Rocchetto, and S. Severini, *New Journal of Physics* **20**, 123030 (2018).
- [38] T. Giordani, E. Polino, S. Emiliani, A. Suprano, L. Innocenti, H. Majury, L. Marrucci, M. Paternostro, A. Ferraro, N. Spagnolo, and F. Sciarrino, *Phys. Rev. Lett.* **122**, 020503 (2019).
- [39] T. Giordani, A. Suprano, E. Polino, F. Acanfora, L. Innocenti, A. Ferraro, M. Paternostro, N. Spagnolo, and F. Sciarrino, *Phys. Rev. Lett.* (to appear) (2020).
- [40] J. VanderPlas, *Python Data Science Handbook* (O'Reilly Media, 2016).
- [41] R. S. Sutton and A. G. Barto, *Reinforcement Learning: An Introduction* (The MIT Press Cambridge, Massachusetts, London, England, 2015).
- [42] V. Dunjko and H. J. Briegel, *Rep. Prog. Phys.*, **81**, 074001 (2018).
- [43] F. Marquardt, "Machine learning for physicists," "<https://machine-learning-for-physicists.org>", [Online; accessed April-2019].
- [44] C. Jarzynski, *Phys. Rev. Lett.* **78**, 2690 (1997).
- [45] G. E. Crooks, *Phys. Rev. E* **60**, 2721 (1999).
- [46] S. Deffner and E. Lutz, *Phys. Rev. Lett.* **107**, 140404 (2011).
- [47] S. Deffner and E. Lutz, *Phys. Rev. Lett.* **105**, 170402 (2010).
- [48] S. Deffner and S. Campbell, *Quantum Thermodynamics*, 2053-2571 (Morgan and Claypool Publishers, 2019).
- [49] V. Vedral, *Rev. Mod. Phys.* **74**, 197 (2002).
- [50] M. Nielsen, *Neural Networks and Deep Learning* (Determination Press, 2015).
- [51] P. Talkner, E. Lutz, and P. Hänggi, *Phys. Rev. E* **75**, 050102 (2007).
- [52] L. Mazzola, G. De Chiara, and M. Paternostro, *Phys. Rev. Lett.* **110**, 230602 (2013).